The significance of the piezoelectric coefficient $d_{31,eff}$ determined from cantilever structures

2013 J. Micromech. Microeng. 23 025008

(http://iopscience.iop.org/0960-1317/23/2/025008)

J. Micromech. Microeng. **23** (2013) 025008 (7pp) doi:10.1088/0960-1317/23/2/025008

The significance of the piezoelectric coefficient $d_{31,\mathrm{eff}}$ determined from cantilever structures

M Dekkers[1,2], H Boschker[1], M van Zalk[1], M Nguyen[1,2,3], H Nazeer[2], E Houwman[2] and G Rijnders[2]

[1] SolMateS BV, Drienerlolaan 5 (bldg 46), 7522-NB, Enschede, The Netherlands
[2] Faculty of Science and Technology, MESA+ Institute for Nanotechnology, University of Twente, PO Box 217, 7500-AE Enschede, The Netherlands
[3] International Training Institute for Materials Science (ITIMS), Hanoi University of Science and Technology, No 1 Dai Co Viet road, Hanoi, Vietnam

E-mail: matthijn.dekkers@solmates.nl

Received 27 July 2012, in final form 22 November 2012
Published 21 December 2012
Online at stacks.iop.org/JMM/23/025008

Abstract
The method used by SolMateS to determine the effective piezoelectric coefficient $d_{31,\mathrm{eff}}$ of $Pb(Zr,Ti)O_3$ (PZT) thin films from cantilever displacement measurements is described. An example from a 48 cantilever dataset using different cantilever widths, lengths and crystal alignments is presented. It is shown that for the layer stack of our cantilevers, the multimorph model is more accurate compared to the bimorph model for the $d_{31,\mathrm{eff}}$ determination. Corrections to the input parameters of the model are further applied in order to reduce the geometrical error of the cantilever that is caused by its design and processing, as well as correction to the measured tip displacement caused by resonance amplification. It is shown that after these corrections, the obtained $d_{31,\mathrm{eff}}$ values are still up to 10% uncertain as the plate behavior and the non-constant radius of curvature of the cantilevers lead to inconsistent results. We conclude that quantitative determination of $d_{31,\mathrm{eff}}$ from the cantilevers is highly subjective to misinterpretation of the models used and the measurement data. The true value of $d_{31,\mathrm{eff}}$ was determined as -118.9 pm V^{-1}.

(Some figures may appear in colour only in the online journal)

1. Introduction

Thin film piezoelectric micro-electromechanical systems (MEMS) have received increased attention in recent years. Bio-sensors, ultrasonic transducers, micro pumps, accelerometers and energy harvesters are only a few examples of novel applications in many different fields. In most of these MEMS devices the piezoelectric effect is used for sensing and actuation purposes. Among piezoelectric thin film materials, $Pb(Zr,Ti)O_3$ (PZT) is the best candidate because of its superior piezoelectric properties. For the use of PZT thin films in MEMS applications, accurate information is needed on its piezoelectric behavior.

The piezoelectric coefficient d_{31} is an important input parameter for the design and simulation of thin film MEMS devices. Other than bulk piezo ceramics, thin piezoelectric films are clamped to the underlying substrate, reducing d_{31} to the 'effective piezoelectric coefficient' $d_{31,\mathrm{eff}}$. Many methods have been employed for either direct or indirect experimental determination of $d_{31,\mathrm{eff}}$, of which the cantilever method is a popular technique due to its attributed simplicity [1]. The preferred routine is to determine the $d_{31,\mathrm{eff}}$ from the dynamic displacement of fabricated cantilever structures upon actuation, as this method approaches the working condition of actual devices. Although the sensitivity is very high, this technique also has its shortcomings. For calculating $d_{31,\mathrm{eff}}$ from the displacement, a model of the mechanical properties of the cantilever is required. As the values for $d_{31,\mathrm{eff}}$ depend on the used model and its input parameters, especially Young's moduli, a one-to-one comparison of the results throughout

the literature is not justified. An accurate determination of the $d_{31,\text{eff}}$ value is required to reduce the discrepancy between simulation and real actuation of a MEMS device regardless of the dimensions, geometry and thin film stack.

Here, we outline the method used by SolMateS in order to clarify the significance of the published $d_{31,\text{eff}}$ values determined from the dynamic cantilever actuation. We discuss the difference between the commonly used heterogeneous bimorph model and the multimorph model, which also takes the effect of the buffer and electrode layers into account. We also describe the corrections applied to $d_{31,\text{eff}}$ that are caused by analytical errors and the change of dimensions of the layers due to device processing. Although all these corrections are applied for $d_{31,\text{eff}}$ determination, we show that the inconsistencies of the model still impede further accuracy of results from the data set.

2. Experimental

The cantilever structures were fabricated using a 4 inch silicon-on-insulator (SOI) wafer. The wafer was coated with a 500 nm buffer layer of SiO_2 by wet oxidation. The 100 nm platinum (Pt) bottom electrode was sputter deposited on an ultrathin titanium adhesion layer. Onto this Pt coated SOI, a 1 μm thick Pb(Zr,Ti)O_3 (PZT) layer was deposited using a large area pulsed laser deposition tool. This tool, developed by SolMateS, is capable of depositing (0 0 1) textured PZT films with a thickness homogeneity <5% on wafers up to 8 inches. The composition of the used PZT is close to the morphotropic phase boundary. The PZT layer was covered by a 100 nm Pt top electrode using sputter deposition. The wafer was further processed into MEMS structures and diced into 12 separate pieces. The processing details are discussed elsewhere [2, 3]. Each 2 × 2 cm^2 die includes over 100 cantilevers with different dimensions and orientations. The widths of the cantilevers are 50, 100 and 150 μm, the lengths vary from 100–800 μm (increments of 100 μm). The thickness of the Si beam was 7.8 μm, as determined with scanning electron microscopy measurements (SEM) after device fabrication. The cantilevers are aligned parallel to either the Si ⟨1 0 0⟩ or the ⟨1 1 0⟩ crystal direction. As shown in figures 1(*a*) and (*b*), the top electrode does not cover the full area of the cantilever. The distance from the edge of the cantilever to the electrode area is 10 μm over the whole beam surface. This implies that only a part of the PZT is used for the actuation of the cantilever. Displacement measurements were performed using a Polytec laser Doppler vibrometer (LDV). Although the equipment is also capable of measuring static deflection it is outperformed by the dynamic mode in terms of accuracy. A 3 V ac excitation voltage was used at a frequency of 8 kHz. A positive 3 V dc bias was used to ensure unipolar excitation. It must be noted that no poling was applied to the PZT thin film prior to the measurements. For high measurement reproducibility the laser is always positioned on the edge of the top electrode area, which is 10 μm away from the edge of the cantilever. The obtained deflection magnitude corresponds to the applied ac amplitude of 3 V.

3. Theory

In the literature often the heterogeneous bimorph model is used for modeling piezoelectric cantilevers. In this model, the d_{31} coefficient can be calculated using the following formula [4]:

$$\delta = \frac{3d_{31}s_s s_p t_s (t_s + t_p) L^2 V}{s_s^2 t_p^4 + 4 s_s s_p t_s t_p^3 + 6 s_s s_p t_s^2 t_p^2 + 4 s_s s_p t_s^3 t_p + s_p t_s^4} \tag{1}$$

in which δ is the cantilever displacement, s_s and s_p are the mechanical compliances of the substrate and the PZT, t_s and t_p are the thicknesses of the substrate and the PZT, L is the length of the cantilever and V is the excitation voltage. The compliance is related to the Young's modulus E by $s = 1/E$. The values for the Young's moduli are listed in table 1. Note that the Young's modulus of silicon is anisotropic between the ⟨1 1 0⟩ and ⟨1 0 0⟩ lattice directions. For PZT we use the value of $E = 95.2$ GPa, which was evaluated from the available experimental data by Pertsev *et al* [5]

The main drawback of the bimorph model is that it only considers the cantilever beam material and the piezoelectric layer. Typical MEMS devices consist of additional layers such as diffusion barriers, stress compensation layers and electrodes. To incorporate the effect of these layers in the calculations, the multimorph model, as described by Weinberg, is used [9]. First the neutral axis for the torque of the multilayered structure is calculated:

$$z_M = \frac{\sum_i z_i E_i A_i}{\sum_i E_i A_i} \tag{2}$$

where z_M indicates the z position of the torque neutral axis (z is the direction perpendicular to the beam), the sum is over all the layers in the device stack, z_i is the position of the center of layer i and $A_i = w_i t_i$ is the cross-sectional area of layer i. w is the width of the layer and t is the thickness of the layer. The curvature of the cantilever is then given by:

$$\frac{1}{R} = \frac{E_p Z_p w_p d_{31} V}{\sum_i E_i A_i \left(t_i^2/12 + Z_i^2\right)} \tag{3}$$

with R the radius of curvature, Z_i the position of the center of layer i with respect to the neutral axis and V the applied voltage. The curvature of curve $z(x)$ is expressed as $\mathrm{d}^2z/\mathrm{d}x^2 = 1/R$, in which x is the position along the cantilever. By solving the equation for $x = L$ the tip displacement can be obtained; $\delta = L^2/2R$.

In order to illustrate the difference between the bimorph and multimorph model, the calculated tip displacement of a 500 μm beam using a d_{31} value of -100 pm V^{-1} and a 3 V driving voltage is presented in figure 2. The thicknesses of the layers are as mentioned in table 1, except for the thickness of Si, which is varied. Significant differences in the results are calculated between the two models, especially for thin Si beams. When comparing the effects of the different layers in the stack separately, the effect of the 100 nm top electrode layer on the calculations is the largest (figure 2(*a*)). This is the outermost layer and therefore much more strain is induced in this layer when the cantilever bends. For thin Si beams, the Pt layer dramatically reduces the displacement due to the symmetric sandwiching of the PZT. The SiO_2 has a less

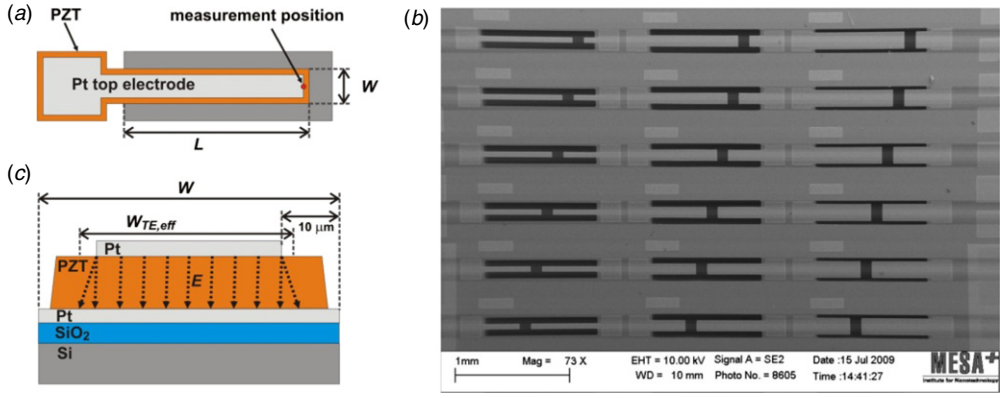

Figure 1. Schematic representation of cantilever (*a*). SEM image of multiple cantilevers showing their different lengths and widths (*b*). Schematic cross section of the cantilever (not to scale) showing the $W_{\mathrm{TE,eff}}$ that actuates the PZT (*c*).

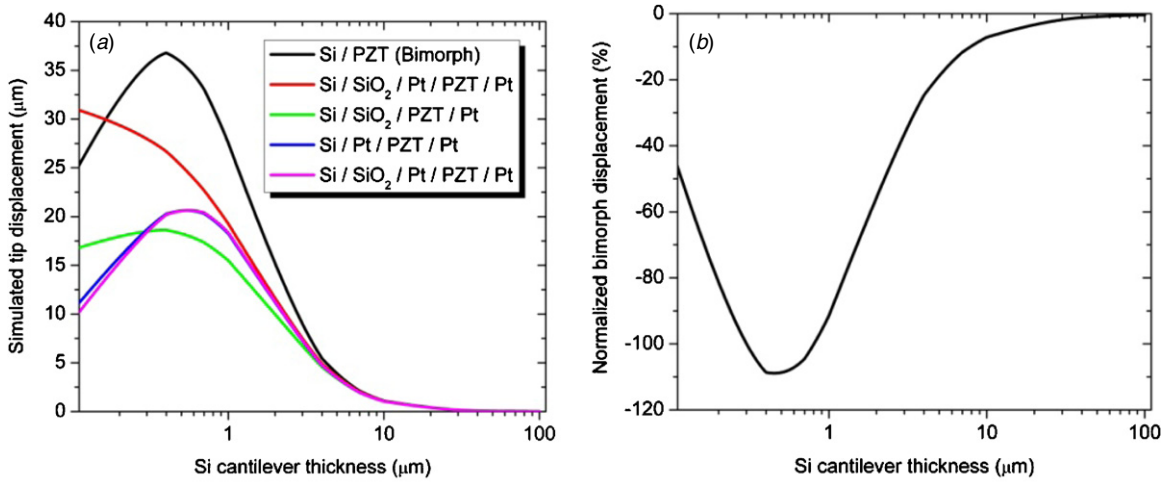

Figure 2. Calculated tip displacement of a 500 μm cantilever using a d_{31} value of -100 pm V^{-1} and a 3 V driving voltage for the bimorph and multimorph models. The influence of the individual layers in the multimorph model is shown by changing the simulated film stack (*a*). Calculated bimorph tip displacement normalized to the calculated displacement by the multimorph model of the complete stack (*b*).

Table 1. Values for materials parameters used [6, 7, 8].

	Si ⟨1 0 0⟩	Si ⟨1 1 0⟩	SiO_2	Pt bottom	PZT	Pt top
E (GPa)	130.2	168.9	70	137.9	95.2	137.9
ρ (kg m^{-3})	2329	2329	2200	21090	7500	21090
ν	0.279	0.064	0.17	0.25	0.35	0.25
t (μm)	7.8	7.8	0.5	0.1	1	0.1
w (μm)	W	W	W	W	$W - 10$	$W - 20$

significant effect than expected because the layer not only adds to the bending moment of inertia, but also results in less bending strain in the Si due to the spacing created between Si and PZT. If the SiO_2 as well as both Pt layers are not taken into account in the multimorph model, the calculated tip displacement coincides with the bimorph model as expected (not shown). In figure 2(*b*), the normalized difference in tip displacement between the two models is shown. For thick Si beams (>10 μm) the difference is not pronounced. However, for beam thicknesses smaller than 10 μm the discrepancy of the two models increases rapidly up to about 100% at 1 μm. This means that the $d_{31,\mathrm{eff}}$ value calculated from the measured tip deflection is significantly underestimated if the bimorph model is used. The used Si beam thickness of 7.8 μm in our devices is small enough to cause an error of about 10% for the bimorph model. Therefore, only the multimorph model is used for the calculations further throughout this paper.

4. Results and discussion

A representative set of 48 cantilevers was measured on a single die resulting in unique cantilevers, as all possible combinations of the length, width and crystal orientation is present in the data set. All devices were functional and were included in the analysis. The displacement was measured three times for each cantilever and the average value was used in the calculations. Figure 3 shows the displacement of the cantilevers sorted by length, width and crystal orientation. The displacement

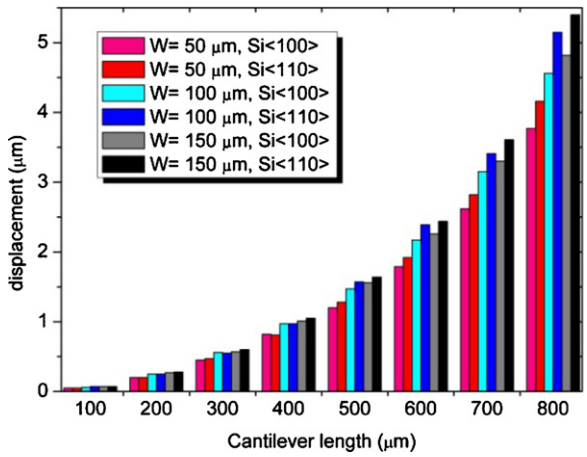

Figure 3. An overview of the tip displacement of the various cantilevers sorted by width, length and crystal orientation.

increases for longer tip lengths as expected. On average the beam displacement was 5% larger for cantilevers along the Si ⟨1 0 0⟩ direction. This is qualitatively (but not quantitatively, as discussed further on) understood by silicon's lower Young's modulus along the ⟨1 0 0⟩ direction, resulting in beams that are less stiff compared to those along Si ⟨1 1 0⟩. An increase of the displacement with the increasing width was also observed. This is attributed to the incomplete area coverage of the top electrode, which is more significant for cantilevers with smaller widths.

From the measured tip displacement, expressed as $\delta = L^2/2R$, combined with equation (3), the value $d_{31,\mathrm{eff}}$ can be obtained. Figure 4(*a*) shows the calculated $d_{31,\mathrm{eff}}$ values using the multimorph model for each cantilever. The anisotropic Young's modulus of Si has been incorporated in the calculations. Although the displacement for beams along Si ⟨1 0 0⟩ is larger, the $d_{31,\mathrm{eff}}$ values are consistently lower compared to those along ⟨1 1 0⟩ crystal orientation. Also a significant spread in $d_{31,\mathrm{eff}}$ with respect to the cantilever width is observed. Furthermore, the values are not linearly dependent with respect to the length of the cantilevers. In the next sections we apply corrections to the calculation of $d_{31,\mathrm{eff}}$ that compensate for analytical errors and imperfect device processing.

First the cantilever length that is used in the calculations needs to be considered. As mentioned, the LDV measurements are performed with the laser positioned at 10 μm from the edge of the tip. On the other hand, an unavoidable undercut during the etching of the silicon in the fabrication process results in longer length cantilevers compared to the design. Earlier we found that the undercut is about 5 μm for along Si ⟨1 1 0⟩, whereas it is about 1 μm along the Si ⟨1 0 0⟩ crystal orientation [10]. Therefore $x = L - 5$ μm or $x = L - 9$ μm has to be used in the calculations for cantilevers along ⟨1 1 0⟩ and ⟨1 0 0⟩ respectively. Figure 4(*b*) shows the $d_{31,\mathrm{eff}}$ corrected for the cantilever length, reducing the spread in the data especially for short cantilevers.

A large spread in the data is still observed for cantilevers with equal length but varying width. Next, corrections for the widths of the layers are introduced in the model. As discussed

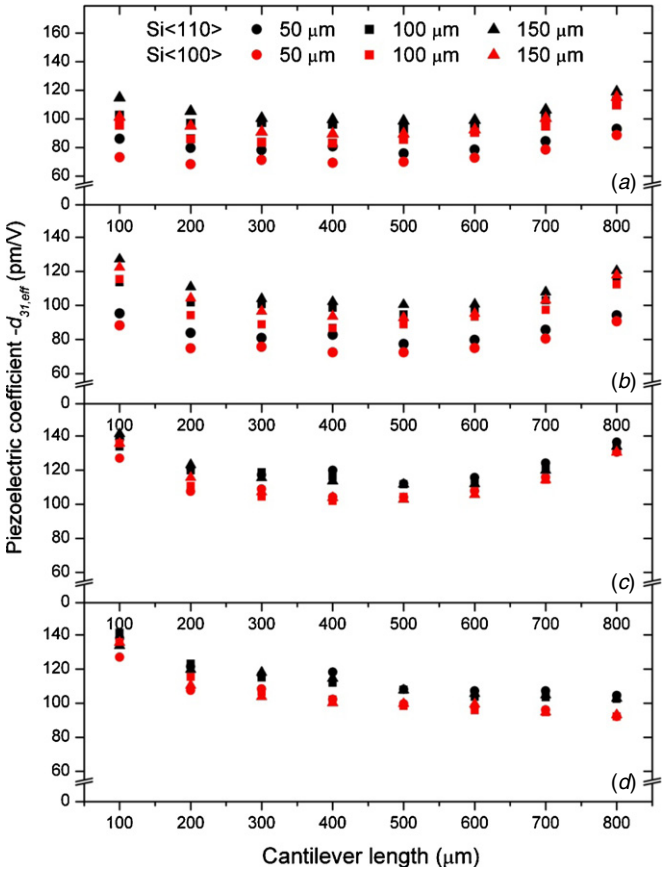

Figure 4. Uncorrected d_{31} values calculated with the multimorph model (*a*). Correction for the length (*b*), width (*c*) and resonance amplification (*d*).

previously, the width of the Pt top electrode is reduced by 20 μm with respect to the width of the cantilever (design of the structure). Also the width of the PZT layer was found to be slightly reduced by 2 μm due to an underetch of the photoresist during the wet chemical etching process. The Young's modulus of PZT and Pt was reduced by the ratio between the width of the material and the cantilever. In addition, a smaller top electrode also means that only part of the PZT on the cantilever is activated. We defined an effective width $W_{\mathrm{TE,eff}}$ which is larger than the width of the top electrode to incorporate the effect of electric field penetration in the PZT outside the top electrode area, as shown in figure 1(*c*). This $W_{\mathrm{TE,eff}}$ is used as a fit parameter to reduce the width dependence in the dataset as much as possible. A value of $W - 17$ μm is obtained for $W_{\mathrm{TE,eff}}$, which implies that 1.5 μm PZT is active outside the top electrode area, which seems a reasonable number considering the 1 μm thick PZT layer. The resulting $d_{31,\mathrm{eff}}$ values, taking the width correction into account, are shown in figure 4(*c*).

The increase in the observed $d_{31,\mathrm{eff}}$ for long cantilevers can be attributed to the dynamic deflection measurement. Ideally the tip displacement should be measured quasistatically or at least well below the resonance frequency of the device. The resonance frequencies range from approximately 1 MHz for the $L = 100$ μm devices to 20 kHz for the $L = 800$ μm devices. Since the measurement frequency is 8 kHz, a significant resonant amplification of the displacement is expected for the

long cantilevers, which requires correction. The magnification factor is based on the amplitude transfer function for a driven harmonic oscillator. For these cantilevers, the quality factor has earlier been determined to be above 250 in all cases [2]. Therefore the correction for displacement is calculated for an oscillator without damping from $M = (1 - (f/f_{\text{res}})^2)^{-1}$. The resonance frequency for all devices is calculated using the analytical relation [11]:

$$f_{\text{res}} = \frac{C^2 t}{2\pi L^2}\sqrt{\frac{E_{\text{eff}}}{12\rho_{\text{eff}}}} \tag{4}$$

with $C = 1.875$ a constant for the fundamental resonance frequency, t the device thickness, E_{eff} the effective Young's modulus of the device (a weighted average of the layer components also depends on the cantilever orientation) and ρ_{eff} the effective density of the device (a weighted average of the layer components). For some 800 μm cantilevers, f_{res} was also measured using the LDV and compared to the calculated values. The difference was in the order of only a few per cent, confirming the validity of the input parameters and the previous corrections. Using the displacement correction factor, the obtained $d_{31,\text{eff}}$ values are presented in figure 4(*d*). It is clear that the initially calculated $d_{31,\text{eff}}$ was overestimated for long cantilevers, as this correction levels the values from $L = 400$ to 800 μm.

The absolute values of $d_{31\text{eff}}$ may be affected by uncertainty in the input parameters of the model. The most obvious errors are those of layer thicknesses and the Young's moduli. Except for ultrathin cantilevers (<1 μm), the thickness error of the silicon beam is by far more significant compared to the other layers. Therefore, we have chosen to check the Si thickness by SEM rather than using the specified device layer thickness of the SOI supplier, which can vary between ± 1 μm across the wafer. The thickness measurement with the SEM results in an estimated error of 2% in the thickness, which can result in an uncertainty of the $d_{31\text{eff}}$ values by almost 5%.

The Young's moduli of silicon are very well known [6]. This is less the case for Pt and SiO_2, but their contribution to the error in the $d_{31\text{eff}}$ value is very small. It is the Young's modulus of PZT that is the most significant, as a 10% higher value yields an 8% lower $d_{31\text{eff}}$. It is not straightforward to obtain a generic E-value for thin film PZT, as it is not only dependent on the deposition method but on thin film composition, structural properties, residual strain and not the least, an appropriate method of determination as well. That is why a wide range values, as for example in [12], from $s^{-1}{}_p = 37$ to 400 GPa is found in the literature. As often it is instead very tempting for authors to use Berlincourt's polycrystalline MPB bulk ceramic value of $E = 72.5$ GPa [13], with respect to $d_{31\text{eff}}$ determination as is, boosts the outcome. From reports over the last decade, it has become evident that the Young's modulus of PZT thin films with MPB composition should be near 100 GPa [12]. Our specific choice for $E = 95.2$ GPa as reported by Pertsev *et al* [5] is based on the fact that our PZT ferro- and piezoelectric data fit very well the thin film phase diagrams presented in this work [14]. Furthermore, we determined the Young's modulus of our PLD deposited films on similar cantilevers earlier, as presented here from the resonance frequency shift [10]. The obtained value of $E = 99$ GPa is very close and further strengthens the validity of the Young's modulus used in this work.

Table 2. Values for $-d_{31,\text{eff}}$ (pm V^{-1}) and $-e_{31,\text{eff}}$ (C/N).

	Along Si ⟨1 1 0⟩ 100–800 μm		Along Si ⟨1 0 0⟩ 100–800 μm	
	$-d_{31,\text{eff}}$	$-e_{31,\text{eff}}$	$-d_{31,\text{eff}}$	$-e_{31,\text{eff}}$
Min	102.6	15.1	92.2	13.6
Max	141.4	20.8	135.7	20.0
Mean	114.1	16.8	104.6	15.4
St. dev.	11.2	1.6	12.5	1.8
St. dev. In%	9.8	9.8	11.9	11.9
Counts	24	24	24	24

The corrected values for $d_{31,\text{eff}}$ are summarized in table 2, together with the corresponding values for the transverse piezoelectric coefficient $e_{31,\text{eff}}$. The latter is calculated by $e_{31,\text{eff}} = d_{31,\text{eff}}/(s_p + s_{12})$, in which $s_{12} = -3.7 \times 10^{-12}$ Pa^{-1} [5] The statistical spread between the selected set of cantilevers is still quite large; i.e. 9.8% for Si⟨1 1 0⟩. From the corrected $d_{31,\text{eff}}$ data in figure 4(*d*), it is seen that the 100 μm length cantilevers in particular deviate from the average. For some of these cantilevers, their length is smaller than their width. If these shortest cantilevers are omitted from the data set, the standard deviation already drops to 6.1% for Si⟨1 1 0⟩. In general, one only considers cantilevers with $L \gg W$. The main reason is that zero stress along the width of the cantilever beam is assumed, which results in anticlastic bending due to Poisson coupling. However, since it is clamped at one end, the Poisson deformation is prevented if the beam becomes significantly short. Because of the additional stress along the width of the cantilever, the plate modulus (PM) instead of the beam modulus (BM) approximation should be used in which the Young's moduli and piezoelectric coefficient should be replaced by $E'' = E/(1 - \nu^2)$ and $d_{31}{}'' = d_{31}(1 + \nu)$ respectively [9]. No straightforward quantitative measure to distinguish between the BM and PM approximation solely based on the dimensions of the structure, is available. With respect to the data set presented in this paper, the structures should be considered both as plate and beam; their behavior gradually moves over from one to the other [15]. We verified this by carrying out full 3D finite-element simulations using the COMSOL software package for the dimensions of the Si beams only within our data set. From the simulations, the resonance frequency was obtained and compared to the analytical determined resonance frequencies from equation 4 for both BM ($E'' = E$) and PM ($E'' = E/(1 - \nu^2)$) approximation. In figure 5(*a*), the difference between the analytical and calculated resonance frequencies is shown. The data confirms that the BM is appropriate for our long Si⟨1 0 0⟩ cantilevers as it gives the smallest deviation from the COMSOL simulation. As the beams become shorter, the deviation for BM increases whereas that of the PM decreases, suggesting a gradual change from one into the other. Surprisingly, the difference between BM and PM is very small for cantilevers along Si⟨1 1 0⟩. The anisotropy in both E and ν results in almost similar values for $E'' = 169.6$ GPa and $E = 168.9$ GPa along the ⟨1 1 0⟩ orientation, making it rather

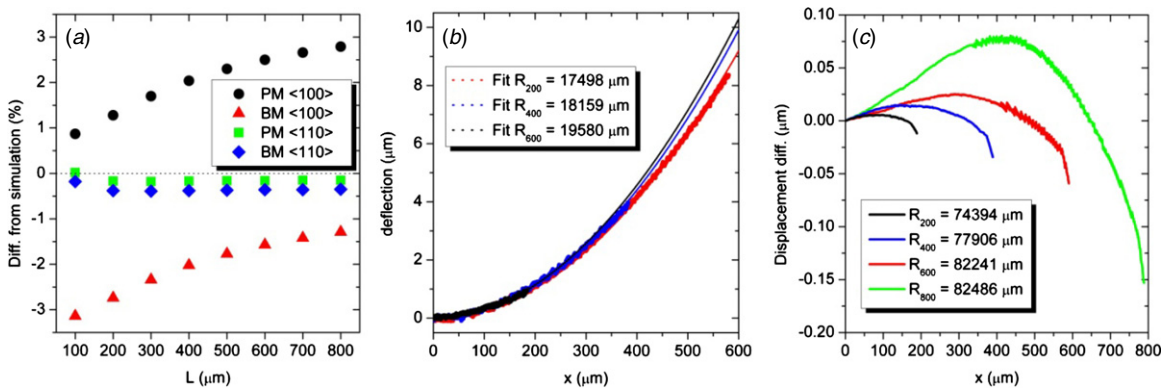

Figure 5. Absolute differences between the analytical and simulated resonance frequencies ($f_{\text{res}}^{\text{AN}}$ and $f_{\text{res}}^{\text{COM}}$) for beam (BM) and plate modulus (PM) of 100 μm wide cantilevers along Si⟨1 0 0⟩ (*a*). Deflection of 200, 400 and 600 μm cantilevers due to pre bending with fitted radius of curvature as specified (*b*). Difference in displacement along the length of the 200, 400, 600 and 800 μm cantilevers (Si⟨1 1 0⟩, $W = 200$ μm) between measured and fitted data with specified radius of curvature (*c*).

independent of the PM or BM approximation. This implies that our data of the ⟨1 0 0⟩ oriented cantilevers is more uncertain. In figure 5(*a*), the deviation for BM <1 0 0> is negative, meaning that the used analytical model underestimates the resonance frequency by a few per cent. As f_{res} is proportional to the square root of E_{eff} equation (4), the calculated $d_{31,\text{eff}}$ values are underestimated even more than this. This mostly explains the lower observed $d_{31,\text{eff}}$ values for ⟨1 0 0⟩ compared to ⟨1 1 0⟩ directions.

A weak aspect of the model to determine $d_{31,\text{eff}}$ is that it assumes a constant radius of curvature R for the actuated cantilever. Using the scanning option of the LDV, the displacement at point x along the length of the cantilevers was measured. A curve with a constant radius was fitted to the data; the difference between measured and fitted data is shown in figure 5(*c*). It is clear that R is not constant along x since for all cantilevers the radius of curvature is stronger over approximately the first $\frac{3}{4}$ of the cantilever length, whereas over the last $\frac{1}{4}$ the actual displacement drops rapidly compared to the fitted average R. Likely because of drag due to the actuation in air, this effect tends to increase as the cantilever length gets longer, as is observed from the higher fitted R values. Fitting curvature over only the first $\frac{3}{4}$ of the cantilever displacement yields R values that are much closer to each other. In particular, the last 20 μm of the electrode covered area on the cantilever only weakly contributes to bending. Because of the discontinuity of the edge of the top electrode, the displacement difference drops off rapidly at the tip end. Best fitting results were obtained on the 400 μm cantilever. This fitted R is a more representative value for the calculation of $d_{31,\text{eff}}$ compared to the displacement of the tip end. According to the fit, the tip displacement, hence $d_{31,\text{eff}}$ was underestimated by 3.8%.

Finally, we discuss the effect of stress in the PZT film caused by the difference in thermal expansion coefficient of PZT and the Si substrate upon cooling after deposition [14]. This residual stress of about 100 MPa results in a tensile strained PZT film that causes the cantilever to bend upward after it is being released during the device fabrication process. In figure 5(*b*), the initial bending measured using white light interferometer of three cantilevers, is shown together with the fitted curve with a constant radius. It can be seen that the radius of curvature is lower for longer cantilevers, which might be due to gravitation. Although the difference may seem small, it implies that the strain in the PZT is not uniform among the complete set of cantilevers. As the PZT properties depend strongly on the strain state of the PZT, the $d_{31,\text{eff}}$ can be significantly different [5]. It has been experimentally demonstrated that a change in the (pre-) strain of PZT results in increased piezoelectric properties [14,16].

Based on the corrections described in this paper, we obtained a nearly uniform relative $d_{31\text{eff}}$ value for a large data set of different cantilevers with different geometries. A uniform value, independent of cantilever geometry, should be expected as the individual layer thicknesses and material properties are the same for each device. Especially since all the cantilevers are located on a small area on the same die. Still a scatter in the data remains because of uncertainties in the application of the model and the strain in the PZT. Taking these considerations into account, the calculated $d_{31,\text{eff}}$ of the 400 μm long and 100 μm wide cantilever aligned along Si⟨1 1 0⟩ is believed to yield the most reliable value from this data set. The value of $d_{31,\text{eff}} = -118.9$ pm V^{-1} is close to the mean value of the complete ⟨1 1 0⟩ data set.

5. Conclusions

The true piezoelectric coefficient of SolMateS' PZT material in cantilever devices is determined to be $d_{31\text{eff}} = -118.9$ pm V^{-1}. We have shown that accurate $d_{31,\text{eff}}$ determination using dynamic actuated cantilever devices is only possible if there is enough understanding about the following.

Model: it is shown that the bimorph model is in general not accurate enough. Especially for thin beams, the multimorph mode is the best approximation. However, both models rely on the assumptions of a constant radius of curvature, which is in general not the case. Furthermore, it should be clear whether it is valid to use the beam or PM.

Geometry: the final geometry of the cantilever is affected by post processing of the devices. This not only counts for the beam material, but for the complete film stack as each individual layer contributes to the cantilever response. Especially for thinner beams, this individual contribution can be significant. Therefore, the exact thickness and size of each layer is an important input parameter for $d_{31,\text{eff}}$ determination.

Measurement: dynamic displacement measurements can be very accurate. However, the measurement frequency should be far enough from the resonance frequency of the device. Otherwise corrections should be applied to the deflection.

Young's modulus: the multimorph model requires the input of the Young's modulus for each layer. The value for PZT in particular is important. A number taken from the literature without consideration is a non-educated guess, as in most cases it does not represent the PZT material used.

Strain: it must be mentioned that once the $d_{31,\text{eff}}$ is determined, it is only valid for the specific PZT material in the tested device. Although the PZT thin film may be one and the same, the locally determined $d_{31,\text{eff}}$ only represents that value for the complete film provided the strain is uniform. The same PZT with a different strain, for example induced by the initial bending of cantilever beams, may yield dissimilar $d_{31,\text{eff}}$.

With respect to reported $d_{31,\text{eff}}$ determination from cantilever displacement, it appears that at least one of the above aspects is not taken into account. This means that the significance of the reported $d_{31,\text{eff}}$ values throughout the literature is, to a certain extent, questionable.

Acknowledgments

The authors gratefully acknowledge the support of the SmartMix Programme of the Netherlands Ministry of Economic Affairs and the Netherlands Ministry of Education, Culture and Science.

References

[1] Liu J -M, Pana B, Chana H L W, Zhua S N, Zhua Y Y and Liu Z G 2002 Piezoelectric coefficient measurement of piezoelectric thin films: an overview *Mater. Chem. Phys.* **75** 12–8

[2] Nguyen M D, Nazeer H, Karakaya K, Pham S V, Steenwelle R, Dekkers M, Abelmann L, Blank D H A and Rijnders G 2010 Characterization of epitaxial $Pb(Zr,Ti)O_3$ thin films deposited by pulsed laser deposition on silicon cantilevers *J. Micromech. Microeng.* **20** 085022

[3] Nazeer H, Nguyen M D, Woldering L A, Abelmann L, Rijnders G and Elwenspoek M E 2011 Determination of the Young's Modulus of pulsed laser deposited epitaxial PZT thin films *J. Micromech. Microeng.* **21** 074008

[4] Smits J and Choi W 1991 The constituent equations of piezoelectric heterogeneous bimorphs *IEEE Trans. Ultrason. Ferroelectr. Freq. Control* **38** 256

[5] Pertsev N A, Kukhar V G, Kohlstedt H and Waser R 2003 Phase diagrams and physical properties of single-domain epitaxial $Pb(Zr_{1-x},Ti_x)O_3$ thin films *Phys. Rev.* B **67** 054107

[6] Brantley W 1973 Calculated elastic-constants for stress problems associated with semiconductor devices *J. Appl. Phys.* **44** 534

[7] Information about thermal wet-grown SiO_2 www.memsnet.org

[8] Salvadori M, Brown I, Vaz A, Melo L L and Cattani M 2003 Measurement of the elastic modulus of nanostructured gold and platinum thin films *Phys. Rev.* B **67** 153404

[9] Weinberg M S 1999 Working equations for piezoelectric actuators and sensors *J. Microelectromech. Syst.* **8** 529–33

[10] Nazeer H, Woldering L A, Abelmann L, Nguyen M D, Rijnders G and Elwenspoek M C 2011 Influence of silicon orientation and cantilever undercut on the determination of the Young's modulus of thin films *Microelectron. Eng.* **88** 2345–48

[11] Volterra E and Zachmanoglou E C 1965 *Dynamics of Vibrations* (Columbus, OH: CE Merrill Books)

[12] Deshpande M and Saggere L 2007 PZT thin films for low voltage actuation: fabrication and characterization of the transverse piezoelectric coefficient *Sensor Actuators A* **135** 690–9

[13] Berlincourt D A, Cmolik C and Jaffe H 1960 Piezoelectric properties of polycrystalline lead titanate zirconate compositions *Proc. IRE* **48** 220–9

[14] Nguyen M D, Dekkers M, Houwman E, Steenwelle R, Wan X, Roelofs A, Schmitz-Kempen T and Rijnders G 2011 Misfit strain dependence of ferroelectric and piezoelectric properties of clamped (0 0 1) epitaxial $Pb(Zr_{0.52},Ti_{0.48})O_3$ thin films *Appl. Phys. Lett.* **99** 252904

[15] Kaldor S K and Noyan I C 2002 Differentiating between elastically bent rectangular beams and plates *Appl. Phys. Lett.* **80** 2284

[16] Prume K, Muralt P, Schmitz-Kempen T and Tiedke S 2007 Tensile and compressive stress dependency of the transverse (e31,f) piezoelectric coefficient of PZT thin films for MEMS devices *Proc. SPIE* **6526** 65260G